Stability analysis of a plane Couette flow of an UCM liquid

J. V. Valério, juvianna@mec.puc-rio.br
M. S. Carvalho, msc@mec.puc-rio.br
Department of Mechanical Engineering, PUC-Rio.

C. Tomei, carlos@mat.puc-rio.br
Department of Mathematics, PUC-Rio, Rua Marques de Sao Vicente 225, Gavea, Rio de Janeiro, RJ, 22453-900, Brazil.

Abstract. *The complete understanding of viscoelastic flows in many situations requires not only the steady state solution of the governing equations, but also its sensitivity to small perturbations. Linear stability analysis leads to a generalized eigenvalue problem, GEVP. Solving the GEVP is challenging, even for Newtonian liquids, because the incompressibility constraint creates singularities that lead to nonphysical eigenvalues at infinity. For viscoelastic flows, the difficulties are even higher because of the continuous spectrum of eigenmodes associated with differential constitutive equations.*
The Couette flow of UCM liquids has been used as a classical problem to address some of the important issues related to stability analysis of viscoelastic flows. The spectrum consists of two discrete eigenvalues and a continuous segment of eigenvalues with real part equal to -1/We (We is the Weissenberg number). Most of the numerical approximation of the spectrum of viscoelastic Couette flow presented in the literature were obtained using spectral expansions. The eigenvalues close to the continuous part of the spectrum show very slow convergence.
In this work, the linear stability of Couette flow of UCM liquid was studied using finite element method, which makes it easier to extend the analysis to complex flows. A new procedure to eliminate the eigenvalues at infinity from the GEVP that come from differential equations without a inertial term (continuity, momentum with Re=0 and the UCM constitutive equation) is also proposed. The procedure takes advantage of the structure of the matrices involved and avoids the computational effort of common mapping techniques. With the proposed procedure, the GEVP is transformed into a smaller simple EVP, making the computations more efficient. Reducing the computational memory and time.
Keywords: *eigenvalues, stability analysis, matrix transformation, incompressible flows.*

1. INTRODUCTION

Linear stability analysis of incompressible flows is used in many practical examples to determine the parameters at which the flow becomes unstable. It is an essential ingredient of the full understanding of many manufacturing processes, where a steady state flow is crucial for uniform product quality. The stability limits of the flow may determine bounds for the operability limits of the process.

In a laminar flow, the stability may be determined by slightly disturbing the flow and tracking the fate of that disturbance. It may die away, persist as a disturbance of similar magnitude, or grow indefinitely leading to a different laminar flow state, to a transient flow, or even to a turbulent flow. The discretization of the system of linear differential equations that describe the amplitude of the perturbations and its rate of growth leads to a non-hermitian, generalized eigenvalue problem (GEVP) of the form $\mathbf{Jc} = \sigma\mathbf{Mc}$, where the eigenvalue σ is the growth rate of disturbances. $\mathbf{J}$ and $\mathbf{M}$ are usually referred to as the *Jacobian* and *Mass matrices*.

The challenges of linear stability analysis of viscoelastic flows are many. The presence of elastic stress boundary layers requires extremely refined mesh in some regions of the flow, leading to very large matrices. Moreover, the differential models used to describe the viscoelastic behavior of liquids lead to singularities. In contrast to Newtonian flows, the linear eigenvalue problem governing the stability of viscoelastic flows involves continuous spectra in addition to discrete eigenvalues.

These difficulties are present even in the stability analysis of simple Couette flow of an upper convected Maxwell liquid. Gorodtsov and Leonov,(1967) presented a theoretical analysis of this problem. They showed that the spectrum is composed by two discrete eigenvalues, usually referred to as the Gorodtsov-Leonov eigenvalues, and a continuous set given by $-1/We \pm i\alpha U$, where We is the Weissenberg number, α is the wavenumber of the perturbation along the flow direction and U is the wall velocity. Since then, there are many examples in the literature trying to recover numerically their predictions and generalizing the studies to different rectilinear flows, such as Poiseuille and multilayered flows, and more elaborate constitutive models. Examples of these efforts include important contributions from Renardy and Renardy (1986), Sureshkumar and Beris, (1995), Sureshkumar *et. al.*, (1999), Wilson *et. al.*, (1999), Grillet *et. al.*, (1999), Sureshkumar and Arora, (2002). In these analysis, the description of the flow perturbation along the cross-stream direction is written in terms of stream functions and spectral methods is used to solve the governing equations. The numerical predictions recover very well the two discrete eigenvalues but approximate the straight line of the continuous part of the spectrum by oval-shaped figures. The width of the oval figure falls as the level of discretization rises, but the convergence is very slow, as it can be seen in Sureshkumar and Beris , (1995), Wilson *et. al.*, (1999), and Sureshkumar

et. al., (1999). As discussed by several authors, the inaccurate approximation of the continuous part of the spectrum and the slow convergence of these eigenmodes are related to the singular nature of the eigenfunction. Kupferman (2005) derived an analytical expression for the singular eigenmodes. They are a family of distribution-valued function for the stress, consisting of delta functions and their derivatives. The oval-shaped figure around the continuous segment can lead to incorrect predictions about the stability of the flow. At high Weissemberg numbers, the real part of eigenvalues in the continuous segment are small negative numbers but their representation in the oval-figure can cross the imaginary axis erroneously. Kupferman (2005) showed the effect of different finite-difference discretization schemes on the numerical prediction of the continuous part of the spectrum.

Finding the solution of the GEVP is extremely challenging even for a viscous flows. The level of discretization needed to describe the perturbed fields is very high, leading to large matrices. The large dimension of the problem rules out the calculation of the full spectrum. Only the leading eigenvalues, those with the largest real part, are calculated. Iterative methods have to be used to compute the relevant part of the spectrum. Moreover, the mass matrix $\mathbf{M}$, which is associated with the transient terms of the governing equations, is singular. Because the mass conservation equation of incompressible flows and the momentum balance equation of a inertialess flows do not have a transient term. This singularity gives rise to infinite eigenvalues. The presence of these very large eigenvalues represents an important difficulty in solving this class of problem, because most iterative methods favor the eigenvalues with the largest modulus, not those with the largest real part. Therefore, the nonphysical infinite eigenvalues should be eliminated before the solution of the eigenproblem, otherwise they would be the first ones to be computed.

In this work, both of the issues discussed before are examined. The linear stability analysis of Couette flow of an Upper-Convected Maxwell liquid is formulated in terms of the primitive variables. The differential equations are discretized using Galerkin's method and finite element basis functions. The finite element method was chosen in order to be able to extend, in the future, the methodology to complex geometries.

A new procedure for the solution of the GEVP is proposed. Realization on how incompressibility and creeping flow lead to infinite eigenvalues and analysis of the structure of the mass and jacobian matrices enabled us to eliminate the infinite eigenvalues. As a consequence, the procedure transforms the generalized eigenproblem (GEVP) into a simple eigenproblem (EVP) whose dimension is much smaller than the original one. The proposed method does not include a penalty term in the mass conservation equation and can be extended to any constitutive model. The complete set of eigenvalues of the transformed problem is formed by all the finite eigenvalues of the original generalized eigenproblem. Therefore, the method presented really eliminates the infinite eigenvalue from the problem and also reduces the size of the matrices involved in the calculation. The proposed algorithm reduces not only the memory requirement but also the CPU time needed to compute the leading eigenvalues of incompressible viscoelastic flows.

2. LINEAR STABILITY ANALYSIS

2.1 Formulation

The velocity $\mathbf{v}$ and pressure p fields of steady state, incompressible flow are governed by the continuity and momentum equations:

$$\nabla \cdot \mathbf{v} = 0, \tag{1}$$

$$Re\, \mathbf{v} \cdot \nabla \mathbf{v} = -\nabla p + \nabla \cdot \mathbf{T} = \mathbf{0}. \tag{2}$$

The Reynolds Number $Re \equiv \rho V L/\mu$ characterizes the ratio of inertial to viscous forces; V and L are suitable characteristic values of velocity and length, ρ is the liquid density and μ, the liquid viscosity. And $\mathbf{T}$ is the extra-stress tensor. In order to compare the predictions with previous work in the literature, Gorodtsov and Leonov (1967), the Reynolds Number is zero and the Upper-Convected Maxwell constitutive equation was chosen to represent the viscoelastic behavior of the liquid:

$$\mathbf{T} + We\, \mathbf{T}_{(1)} = \dot{\gamma}, \tag{3}$$

where, $\mathbf{T}_{(1)} = \mathbf{v} \cdot \nabla \mathbf{T} - (\nabla \mathbf{v})\mathbf{T} - \mathbf{T}(\nabla \mathbf{v})^T$ is the upper convected derivative and $\dot{\gamma} = \left(\nabla \mathbf{v} + \nabla \mathbf{v}^T\right)$ is the rate-of-strain tensor. $We \equiv V\lambda/L$ is the Weissenberg number and λ is the relaxation time of the liquid. The gradient of the velocity here is defined as $\nabla \mathbf{v} = \dfrac{\partial v_i}{\partial x_j} e_i e_j$.

The flow geometry and boundary conditions are shown in Fig.1. Liquid flows between two parallel plates located at $y = \pm 1$ that are moving with velocity $U = \pm 1$. Gorodtsov and Leonov (1967) considered the half upper part of this geometry.

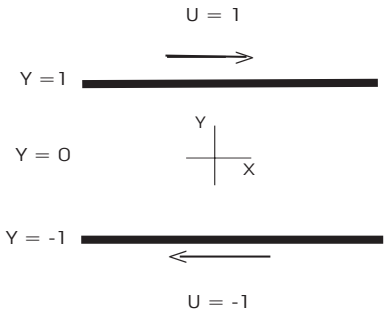

Figure 1. Configuration of plane Couette flow.

The steady state solution of this problem is given by:

$$\mathbf{v_0} = (y, 0, 0), \quad p_0 = 0 \quad \text{and} \quad \mathbf{T}_0 = \begin{bmatrix} 2We & 1 & 0 \\ 1 & 0 & 0 \\ 0 & 0 & 0 \end{bmatrix}. \tag{4}$$

The goal of linear stability analysis is to determine if a steady flow is stable with respect to infinitesimal disturbances. The stability of the flow can be judged by solving the time-dependent system for the long time behavior of infinitesimal perturbations to the base flow. Accordingly, the disturbed fields, i.e. velocity, pressure and stress, are written as the sum of the base state and an infinitesimal perturbation based on normal modes theory

$$\mathbf{v}(\mathbf{x}, t) = \mathbf{v_0}(\mathbf{x}) + \epsilon\, \mathbf{v}'(y) e^{i\alpha x + \sigma t}, \tag{5}$$

$$p(\mathbf{x}, t) = p_0(\mathbf{x}) + \epsilon\, p'(y) e^{i\alpha x + \sigma t}, \tag{6}$$

$$\mathbf{T}(\mathbf{x}, t) = \mathbf{T}_0(\mathbf{x}) + \epsilon\, \mathbf{T}'(y) e^{i\alpha x + \sigma t}, \tag{7}$$

$\mathbf{v_0}$, p_0 and $\mathbf{T}_0$ are the velocity, pressure and stress fields of the base flow, known *a priori* and showed in eq.(4). $\mathbf{v}'$, p' and $\mathbf{T}'$ are the fields that describe the amplitude, α the wave number along the flow direction and σ is the growth factor of the perturbation. If $\Re(\sigma) < 0$ ($\Re$ denotes the real part), the perturbation dies and the flow is said to be stable. If $\Re(\sigma) > 0$, the disturbance grows with time and the flow is said to be unstable .

Thus, the velocity $\mathbf{v}$, pressure p and stress $\mathbf{T}$ of the disturbed flow are governed by a time-dependent system:

$$\nabla \cdot \mathbf{v} = 0, \tag{8}$$

$$-\nabla p + \nabla \cdot \mathbf{T} = \mathbf{0}, \tag{9}$$

$$\mathbf{T} + We\, \mathbf{T}_{(1)} = \dot{\gamma}, \tag{10}$$

where, $\mathbf{T}_{(1)} = \dfrac{\partial \mathbf{T}}{\partial t} + (\mathbf{v} \cdot \nabla)\mathbf{T} - (\nabla \mathbf{v})\mathbf{T} - \mathbf{T}(\nabla \mathbf{v})^T$ is the upper convected derivative adding a transient term.

Modifications on the equation system that describe the convection and diffusion of momentum in flow of viscoelastic liquids have been proposed in recent years with the goal of stabilizing the computation methods used to solve it. As suggested by Szady *et. al.* (1995), an additional variable $\mathbf{G}$ is introduced to represent the velocity gradient as an independent field. In an incompressible liquid it should be traceless because of $\nabla \cdot \mathbf{v} = 0$. Pasquali and Scriven (2002) found that a suitable means of enforcing this is with the equation

$$\mathbf{G} - \nabla \mathbf{v} + \frac{(\nabla \cdot \mathbf{v})\mathbf{I}}{tr(\mathbf{I})} \tag{11}$$

Thus, the modified system of equations of creeping flow of a UCM liquid are:

$$\begin{aligned} &\nabla \cdot \mathbf{v} = 0, \\ &-\nabla p + \nabla \cdot \mathbf{T} = \mathbf{0}, \\ &\mathbf{T} + We\, \left[\mathbf{u} \cdot \nabla \mathbf{T} - (\mathbf{G})\mathbf{T} - \mathbf{T}(\mathbf{G})^T\right] = \left(\mathbf{G} + \mathbf{G^T}\right), \\ &\mathbf{G} - \nabla \mathbf{v} + \frac{(\nabla \cdot \mathbf{v})\mathbf{I}}{tr(\mathbf{I})} = \mathbf{0}. \end{aligned} \tag{12}$$

A system of linear differential equations that describe the perturbed fields and its growth rate is obtained after substituting the perturbed fields, e.g. eqs.(5,6,7), into the modified transient system of equations, eqs.(12), neglecting terms of order $\mathcal{O}(\epsilon^2)$:

Continuity equation:

$$i\alpha u' + \frac{dv'}{dy} = 0; \tag{13}$$

UCM contitutive model:

$$(\sigma We + S)T'_{11} - 2WeT'_{12} - (4We^2 + 2)G_{11} - 2WeG_{12} = 0, \tag{14}$$

$$(\sigma We + S)T'_{12} - WeT'_{22} - WeG_{11} - G_{12} - (2We^2 + 1)G_{21} - WeG_{22} = 0, \tag{15}$$

$$(\sigma We + S)T'_{22} - 2WeG_{12} - 2G_{22} = 0; \tag{16}$$

where $S = [1 + Wei\alpha y]$.

Momentum equations:

$$-i\alpha p' + \frac{dT'_{12}}{dy} + i\alpha T'_{11} = 0, \qquad -\frac{dp'}{dy} + \frac{dT'_{22}}{dy} + i\alpha T'_{12} = 0; \tag{17}$$

Interpolated velocity gradient equations:

$$-\frac{1}{2}i\alpha u' + \frac{1}{2}\frac{dv'}{dy} + G_{11} = 0, \qquad -\frac{du'}{dy} + G_{12} = 0, \tag{18}$$

$$-i\alpha v' + G_{21} = 0 \qquad \frac{1}{2}i\alpha u' - \frac{1}{2}\frac{dv'}{dy} + G_{22} = 0. \tag{19}$$

The boundary conditions are

$$u'(y = \pm 1) = 0, \qquad v'(y = \pm 1) = 0. \tag{20}$$

The unknowns of the problem are the perturbed fields p', $\mathbf{T}'$, $\mathbf{v}'$ and $\mathbf{G}$ and the growth rate of the perturbation σ.

2.2 Discretization by Galerkin's Method and Finite Element Basis Functions

The perturbation fields $p'(y)$, $\mathbf{T}'(y)$, $\mathbf{v}'(y)$ and $\mathbf{G}(y)$ and its rate of growth σ can be found by applying Galerkin's weighted residual method to the systems of equations (13) – (20). The weighting functions used for the momentum equations ϕ_j are piecewise Lagrangian quadratic polynomial functions and for continuity equation χ_j, constitutive equations ψ_j and interpolated velocity gradient equations φ_j are piecewise linear discontinuous polynomial functions.

Once all the variables are represented in terms of the basis functions (u'_h, T'_{11h}, etc.) some of the weighted residual equation of (13) – (19) are:

$$R^j_c = \int_{-1}^{1} \left(i\alpha u'_h + \frac{dv'_h}{dy} \right) \chi_j \, dy \tag{21}$$

$$R^j_{T_{xx}} = \sigma \int_{-1}^{1} (We\, T'_{xxh})\psi_j \, dy \; + \; \int_{-1}^{1} \left(ST'_{xxh} - 2WeT'_{xy_h} - (4We^2 + 2)G_{xxh} - 2WeG_{xy_h} \right) \psi_j \, dy \tag{22}$$

$$R^j_{mx} = \int_{-1}^{1} \left(i\alpha p'_h - i\alpha T'_{xxh} \right) \phi_j \, dy \; + \; \int_{-1}^{1} (T'_{xy_h}) \frac{d\phi_j}{dy} \, dy. \tag{23}$$

$$R^j_{G_{xx}} = \int_{-1}^{1} \left(-\frac{1}{2}i\alpha u'_h + \frac{1}{2}\frac{dv'_h}{dy} + G_{xxh} \right) \varphi_j \, dy \tag{24}$$

where, following Galerkin's method, each perturbed field is approximated with a linear combination of the same basis functions:

$$p'_h = \sum_{k=1}^{m} P_k \, \chi_k, \qquad \mathbf{T}'_h = \begin{bmatrix} T_{11}{}'_h & T_{12}{}'_h \\ T_{12}{}'_h & T_{22}{}'_h \end{bmatrix} = \begin{bmatrix} \sum_{k=1}^{m} T_{11k}\psi_k & \sum_{k=1}^{m} T_{12k}\psi_k \\ \sum_{k=1}^{m} T_{12k}\psi_k & \sum_{k=1}^{m} T_{22k}\psi_k \end{bmatrix}, \tag{25}$$

$$\mathbf{u}'_h = \begin{bmatrix} u'_h \\ v'_h \end{bmatrix} = \begin{bmatrix} \sum_{k=1}^{n} U_k \phi_k \\ \sum_{k=1}^{n} V_k \phi_k \end{bmatrix}, \qquad \mathbf{G}_h = \begin{bmatrix} G_{11h} & G_{12h} \\ G_{21h} & G_{22h} \end{bmatrix} = \begin{bmatrix} \sum_{k=1}^{m} \mathcal{G}_{11k} \varphi_k & \sum_{k=1}^{m} \mathcal{G}_{12k} \varphi_k \\ \sum_{k=1}^{m} \mathcal{G}_{12k} \varphi_k & \sum_{k=1}^{m} \mathcal{G}_{22k} \varphi_k \end{bmatrix}. \quad (26)$$

An integration by parts was necessary to avoid the derivative of the basis function that expand the pressure and the components of stress tensor, into the momentum equations. It is important to notice that the convective term into the constitutive equations for this case, unidimensional flow, is zero. Thus, it was not necessary an integration by parts in these equations.

The number of algebraic equations is $N_{total} = 2n + 8m$, where n is the number of basis functions used to expand each component of the velocity perturbation and m is the number of basis functions used to expand the disturbances of the pressure, the three components of the stress tensor (it is a symmetric tensor) and the four components of the interpolated velocity gradient tensor. In terms of the numbers of elements N, $n = 2N + 1$ and $m = 2N$, as shown in Fig.2.

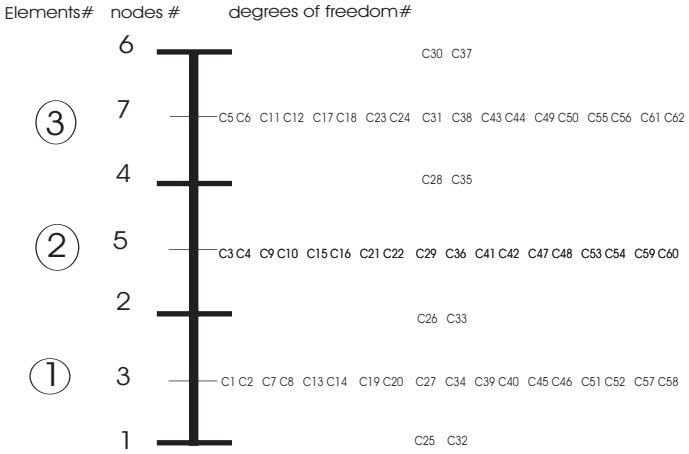

Figure 2. Example of numbering scheme for elements, nodes and degrees of freedom. The first coefficients correspond to pressure field, C1 – C6. The next ones come from stress tensor components, C7 – C24. The coefficients of the velocity field, C25 – C38. Finally, the coefficients related to the velocity gradient components,C39 – C62.

In vector form, the set of algebraic equations is represented by $\mathbf{R}(\mathbf{c}) = \mathbf{0}$, where $\mathbf{c}$ is the column vector of coefficients of the finite element basis function with which the perturbation are represented and $\mathbf{R}$ is the column vector of weighted residual equations. When this set of equations is expanded in Taylor series and truncated at order $\mathcal{O}(\mathbf{c}^2)$ on the grounds that the perturbation is infinitesimal, the result is the equation set $\dfrac{\partial \mathbf{R}}{\partial \mathbf{c}}\,\mathbf{c} = \mathbf{0}$. Where, $\dfrac{\partial \mathbf{R}}{\partial \mathbf{c}} = -\sigma \mathbf{M} + \mathbf{J}$ is the matrix of sensitivities of the weighted residuals with respect to the unknown coefficient of the perturbations and for convenience, it is split in two matrices resulting the generalize non-Hermitian eigenvalue problem:

$$\mathbf{J}\mathbf{c} = \sigma \mathbf{M}\mathbf{c}. \quad (27)$$

The mass matrix $\mathbf{M}$ is singular, it has only one block in the diagonal different from zero. Consequently, the number of eigenvalues of (27) is smaller than the dimension of the problem $N = 2n + 8m$. The missing eigenvalues are commonly referred to as infinite eigenvalues, because if the mass matrix is slightly perturbed to remove the singularity, e.g. $\mathbf{M}^* = \mathbf{M} + \epsilon \mathbf{I}$, large eigenvalues appear in the spectrum, and they grow unbounded as $\epsilon \to 0$.

The expected of the number of infinite eigenvalues is the number of zero's rows and columns in the mass matrix, e.g. $14N + 2$. The method presented in the following section shows that the number of infinite eigenvalues is actual larger than the number of zero's rows and columns in the mass matrix and eliminates the infinite eigenvalue from the problem, transforming the GEVP into a simple EVP.

2.3 Proposed Transformation

Following the ordering scheme explained before, both the mass and jacobian matrices are divided into blocks according to the equivalent residual equations and corresponding degrees of freedom.

$$\mathbf{M} = \left(\begin{array}{c|c|c|c} \mathbf{0} & \mathbf{0} & \mathbf{0} & \mathbf{0} \\ \hline \mathbf{0} & \mathbf{M_{22}} & \mathbf{0} & \mathbf{0} \\ \hline \mathbf{0} & \mathbf{0} & \mathbf{0} & \mathbf{0} \\ \hline \mathbf{0} & \mathbf{0} & \mathbf{0} & \mathbf{0} \end{array}\right) \begin{array}{c} 2N \\ 6N \\ 4N+2 \\ 8N \end{array} \qquad \mathbf{J} = \left(\begin{array}{c|c|c|c} \mathbf{0} & \mathbf{0} & \mathbf{J_{13}} & \mathbf{0} \\ \hline \mathbf{0} & \mathbf{J_{22}} & \mathbf{0} & \mathbf{J_{24}} \\ \hline \mathbf{J_{31}} & \mathbf{J_{32}} & \mathbf{0} & \mathbf{0} \\ \hline \mathbf{0} & \mathbf{0} & \mathbf{J_{43}} & \mathbf{J_{44}} \end{array}\right) \begin{array}{c} 2N \\ 6N \\ 4N+2 \\ 8N \end{array}. \quad (28)$$

N is the number of elements. The dimension of each block is also indicated; for example $[\mathbf{M_{22}}] = 6N \times 6N$, $[\mathbf{J_{32}}] = 4N + 2 \times 6N$.

The eigenvalues σ of the GEVP (27) are the roots of the characteristic polynomial

$$p(\sigma) \equiv \det(\mathcal{A}) \equiv \det(-\sigma\mathbf{M} + \mathbf{J}). \tag{29}$$

Said differently, we are interested in the values of σ for which the homogeneous system $(\mathbf{J} - \sigma\mathbf{M})\mathbf{c} = 0$ has a nontrivial solution. In particular, if one replaces both $\mathbf{J}$ and $\mathbf{M}$ by matrices $\tilde{\mathbf{J}}$ and $\tilde{\mathbf{M}}$, the GEVP $\tilde{\mathbf{J}}\tilde{\mathbf{c}} = \sigma\tilde{\mathbf{M}}\tilde{\mathbf{c}}$ has the same (generalized) eigenvalues as the original system if the corresponding homogeneous system $(\tilde{\mathbf{J}} - \sigma\tilde{\mathbf{M}})\tilde{\mathbf{c}} = 0$ has a nontrivial solution. Convenient modifications are related to the process of solving the homogeneous system above by a two-sided Gaussian elimination, in the sense that row and column operations are allowed: notice that we are not interested in the value of a solution, but just in the existence of a nontrivial one. More algebraically, we consider left and right multiplications of both $\mathbf{J}$ and $\mathbf{M}$ by invertible matrices $\mathbf{X}$ and $\mathbf{Y}$ independent of σ.

The structure of the original matrix $\mathcal{A} \equiv \det(-\sigma\mathbf{M} + \mathbf{J})$ is shown in figure 3.

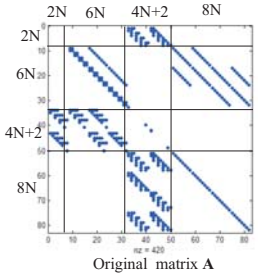

Figure 3. Example of the Structure of the original matrix, with 4 elements, $\mathcal{A} = -\sigma\mathbf{M} + \mathbf{J}$.

The algebraic equations associated with the Dirichlet's boundary conditions do not have a time derivative, and the perturbed velocity field at these boundaries are identically zero. Therefore, eliminating the rows and columns related to these equations and unknowns will not change the roots of the characteristic polynomial $p(\sigma)$. This is the first step in the procedure of eliminating the infinite eigenvalues. Since there are 4 Dirichlet's boundary conditions in the problem, the dimension of the transformed matrix is $20N - 2$, whereas the size of the original matrix $\mathcal{A}$ was $20N + 2$. After eliminating the rows and columns associated with essential boundary conditions, it is also convenient to divide the new matrix $\mathbf{A} \equiv -\sigma\mathbf{M} + \mathbf{J}$ into a different structure of blocks, as shown below.

$$\mathbf{A} = \left(\begin{array}{c|c|c} \mathbf{A_{11}}(\sigma) & \mathbf{A_{12}} & \mathbf{A_{13}} \\ \hline \mathbf{A_{21}} & \mathbf{0} & \mathbf{0} \\ \hline \mathbf{0} & \mathbf{A_{32}} & \mathbf{A_{33}} = \mathbf{D} \end{array}\right) \begin{array}{c} 8N \\ \\ 4N-2 \\ \\ 8N \end{array} \tag{30}$$

On this new partition of the matrix, only the first diagonal block $\mathbf{A_{11}}$ has any contribution from the mass matrix and consequently depend on the growth factor σ. It is important to note that the block $\mathbf{A_{33}}$ is diagonal. The block $\mathbf{A_{32}}$ can be eliminated using the following transformation:

$$\widetilde{\mathbf{A}} = \left(\begin{array}{c|c|c} \mathbf{A_{11}}(\sigma) & \widetilde{\mathbf{A}}_{\mathbf{12}} & \mathbf{A_{13}} \\ \hline \mathbf{A_{21}} & \mathbf{0} & \mathbf{0} \\ \hline \mathbf{0} & \mathbf{0} & \mathbf{D} \end{array}\right) = \mathbf{A}\,\mathbf{T_r}, \quad \text{where} \quad \mathbf{T_r} = \left(\begin{array}{c|c|c} \mathbf{I}_{[8N]} & \mathbf{0} & \mathbf{0} \\ \hline \mathbf{0} & \mathbf{I}_{[4N-2]} & \mathbf{0} \\ \hline \mathbf{0} & -\mathbf{D}^{-1}\mathbf{A_{32}} & \mathbf{I}_{[8N]} \end{array}\right), \tag{31}$$

the transformed matrix is shown in figure 4:

The characteristic polynomial $p_1(\sigma)$ of the transformed matrix $\widetilde{\mathbf{A}}$ is

$$p_1(\sigma) = \det(\widetilde{\mathbf{A}}) = \det(\mathbf{A})\ \det(\mathbf{T_r}) = \det(\mathbf{A}) = p(\sigma). \tag{32}$$

Because the blocks used in the definition of $\mathbf{T_r}$ do not contain the eigenvalue σ, the determinant of this matrix is independent of the eigenvalue. Moreover, the transformation matrix is a triangular matrix with diagonal entries equal to one, therefore its determinant is equal to one. The characteristic polynomial of the transformed matrix $\widetilde{\mathbf{A}}$, $p_1(\sigma)$ is exactly the characteristic polynomial of the original matrix $\mathbf{A}$, $p(\sigma)$; both polynomials have the same roots. The multiplication of $\mathbf{A}$ by $\mathbf{T_r}$ does not change the spectrum of the original problem. It is important to note that the computational cost of this transformation is small, it only requires the inverse of a diagonal matrix and a matrix-matrix multiplication.

The characteristic polynomial $p_1(\sigma)$ can be written as:

$$p_1(\sigma) = \det(\widetilde{\mathbf{A}}) = \det(\left(\begin{array}{c|c|c} \mathbf{A_{11}}(\sigma) & \widetilde{\mathbf{A}}_{\mathbf{12}} & \mathbf{A_{13}} \\ \hline \mathbf{A_{21}} & \mathbf{0} & \mathbf{0} \\ \hline \mathbf{0} & \mathbf{0} & \mathbf{D} \end{array}\right)) = \det(\mathbf{D})\ \det(\left(\begin{array}{cc} \mathbf{A_{11}}(\sigma) & \widetilde{\mathbf{A}}_{\mathbf{12}} \\ \mathbf{A_{21}} & \mathbf{0} \end{array}\right)) = \kappa_1\, p_2(\sigma).$$

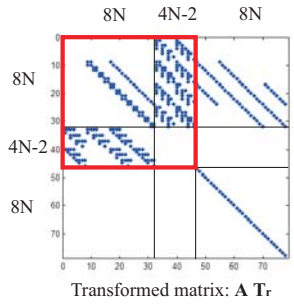

Figure 4. Example of the structure of the matrix, with 4 elements, after been multiplied by $\mathbf{T_r}$ by the right side: $\widetilde{\mathbf{A}} = \mathbf{T_r A}$. The marked block is the relevant one, called $\mathbf{B}$.

Again, because $\mathbf{D}$ is independent of the eigenvalue σ, the characteristic polynomial of the original matrix, $p(\sigma)$, is proportional to the characteristic polynomial $p_2(\sigma)$ of the block $\mathbf{B} = \begin{pmatrix} \mathbf{A_{11}}(\sigma) & \widetilde{\mathbf{A}}_{\mathbf{12}} \\ \mathbf{A_{21}} & \mathbf{0} \end{pmatrix}$.

Consequently, both polynomials have the same roots. The finite eigenvalues of $\mathbf{B}$ are the same as the finite eigenvalues of $\mathbf{A}$.

It is convenient to redivide $\mathbf{B}$, in the following sub-block structure:

$$\mathbf{B} = \left(\begin{array}{c|c|c} \mathbf{B_{11}}(\sigma) & \mathbf{B_{12}}(\sigma) & \mathbf{B_{13}} \\ \hline \mathbf{B_{21}}(\sigma) & \mathbf{B_{22}}(\sigma) & \mathbf{B_{23}} \\ \hline \mathbf{B_{31}} & \mathbf{B_{32}} & \mathbf{B_{33}} = \mathbf{0} \end{array}\right) \begin{array}{c} 4N-2 \\ \\ \\ 4N+2 \\ \\ \\ 4N-2 \end{array} \quad \begin{array}{c} \\ \\ \\ \\ \\ \\ 4N-2 \end{array} \quad \begin{array}{c} \\ \\ \\ \\ \\ \\ 4N+2 \end{array} \quad \begin{array}{c} \\ \\ \\ \\ \\ \\ 4N-2 \end{array} \tag{33}$$

The blocks $\mathbf{B_{23}}$ and $\mathbf{B_{32}}$ can be eliminated by using the following transformations:

$$\widetilde{\mathbf{B}} = \left(\begin{array}{c|c|c} \mathbf{B_{11}}(\sigma) & \widetilde{\mathbf{B}}_{\mathbf{12}}(\sigma) & \mathbf{B_{13}} \\ \hline \widetilde{\mathbf{B}}_{\mathbf{21}}(\sigma) & \widetilde{\mathbf{B}}_{\mathbf{22}}(\sigma) & \mathbf{0} \\ \hline \mathbf{B_{31}} & \mathbf{0} & \mathbf{0} \end{array}\right) = \mathbf{M_l}\,\mathbf{B}\,\mathbf{M_r}, \tag{34}$$

where

$$\mathbf{M_l} = \left(\begin{array}{c|c|c} \mathbf{I}_{[4N-2]} & \mathbf{0} & \mathbf{0} \\ \hline -\mathbf{B_{23}}\mathbf{B_{13}^{-1}} & \mathbf{I}_{[4N+2]} & \mathbf{0} \\ \hline \mathbf{0} & \mathbf{0} & \mathbf{I}_{[4N-2]} \end{array}\right), \qquad \mathbf{M_r} = \left(\begin{array}{c|c|c} \mathbf{I}_{[4N-2]} & -\mathbf{B_{31}^{-1}}\mathbf{B_{32}} & \mathbf{0} \\ \hline \mathbf{0} & \mathbf{I}_{[4N+2]} & \mathbf{0} \\ \hline \mathbf{0} & \mathbf{0} & \mathbf{I}_{[4N-2]} \end{array}\right). \tag{35}$$

The characteristic polynomial $p_3(\sigma)$ of the transformed matrix $\widetilde{\mathbf{B}}$ is

$$p_3(\sigma) = \det(\widetilde{\mathbf{B}}) = \det(\mathbf{M_l})\det(\mathbf{B})\det(\mathbf{M_r}) = \det(\mathbf{B}) = p_2(\sigma). \tag{36}$$

Again, because the blocks used in the definition of $\mathbf{M_l}$ and $\mathbf{M_r}$ do not contain the eigenvalue σ, the multiplication of $\mathbf{B}$ by $\mathbf{M_l}$ and $\mathbf{M_r}$ does not change its spectrum. Moreover, the determinant of the transformed matrix $\widetilde{\mathbf{B}}$ may be computed by permuting rows, so as to interchange the bottom and top row blocks. Indeed, this gives rise to a block triangular matrix, whose determinant, up to sign, equals $\det(\mathbf{B_{13}})\ \det(\mathbf{B_{31}})\ \det(\widetilde{\mathbf{B}}_{\mathbf{22}}(\sigma))$. The upshot is that $p(\sigma)$, the original characteristic polynomial, and $\det(\widetilde{\mathbf{B}}_{\mathbf{22}}(\sigma))$ have the same roots, it is shown in the figure 5.

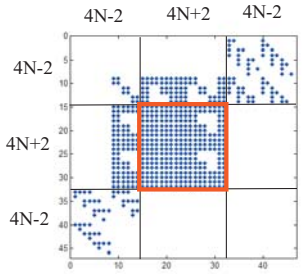

Figure 5. Structure of final transformed matrix $\widetilde{\mathbf{B}} = \mathbf{M_l}\,\mathbf{B}\,\mathbf{M_r}$. The complete finite portion of the eigenspectrum of the original problem is contained in the center $(4N+2) \times (4N+2)$ marked block.

Because the submatrix $\widetilde{\mathbf{B}}_{\mathbf{22}}$ is non-singular, the number of roots of its characteristic polynomial is $4N+2$, the number of finite eigenvalues of the original problem.

The infinite eigenvalues were eliminated by the transformations, so the generalized eigenvalue problem (GEVP) can be transformed into a simple eigenvalue problem (EVP) ($\widetilde{\mathbf{M}}_{\mathbf{22}}$ is not singular):

$$\left(-\sigma\,\widetilde{\mathbf{M}}_{22}+\widetilde{\mathbf{J}}_{22}\right)\mathbf{d}=0 \quad\Rightarrow\quad \underbrace{\widetilde{\mathbf{M}}_{22}^{-1}\widetilde{\mathbf{J}}_{22}}_{\mathbf{E}}\mathbf{d}=\sigma\mathbf{d} \tag{37}$$

The main computational cost of the proposed method corresponds to the cost of inverting two $(4N-2)\times(4N-2)$ matrices to construct the transformation matrices $\mathbf{M_l}$ and $\mathbf{M_r}$, and one $(4N+2)\times(4N+2)$ matrix to find $\widetilde{\mathbf{M}}_{22}^{-1}$. The cost of inverting the diagonal matrix $\mathbf{D}$, used in the definition of $\mathbf{T_r}$, is irrelevant. The benefit of the method is that the complete physically relevant spectrum of the original problem can be evaluated by solving a simple EVP that is approximately 1/5 of the size of the original GEVP using this formulation.

In order to illustrate the structure of the matrices of the process of filtering the infinite eigenvalue, an exemple case with only four finite elements is shown. For this discretization level, the total number of degrees of freedom of the problem is $20N+2=82$. The structure of the non-zero entries of the matrix $\mathcal{A}=-\sigma\mathbf{M}+\mathbf{J}$ is shown in Fig.**??**. After the proposed transformations all the information of the finite portion of the spectrum of the original GEVP is contained in the $(4N+2)\times(4N+2)$ central block of the transformed matrix, 18×18 in this particular case, indicated in the figure 5.

2.4 Results

To compare the spectrum of the plane Couette flow of UCM liquid predicted with the method described here with data available in the literature, the calculations were performed using the same parameters used by Sureshkumar (2004), $We=10$ and $\alpha=1$.

In order to validate the proposed method, the predicted spectrum was compared with the solution of the original generalized eigenproblem using QZ method. The comparison was done with a mesh of 60 elements. The eigenvalues computed with both methods are shown in Fig.6; they coincide up to the 5^{th} decimal figure. The reduced EVP and the original GEVP were solved by the LAPACK routine ZGEEV (for non-hermitian matrix) and in the case of the GEVP, using the QZ method. All calculation were performed on a 1.00 GB of RAM, 789 GHz AMD Turion 64 Mobile processor machine, using MatLab, version 6.5. With 60 elements, the number of degrees of freedom of the problem, i.e. the dimension of the original generalized eigenproblem, is $20N+2=1202$. After using the transformations presented here to eliminate the infinite eigenvalues of the problem, the reduced matrix, that contains all the information of the physically relevant finite portion of the spectrum, has a dimension of $4N+2=242$. The dimension of the reduced eigenvalue problem is approximately $1/5$ of the size of the original generalized eigenproblem. This will lead to enormous reduction of the time necessary to determine the finite eigenvalues of the GEVP.

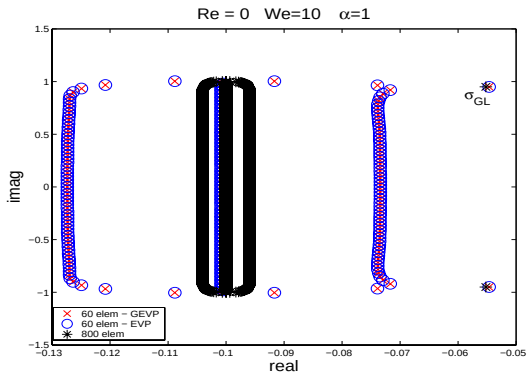

Figure 6. Spectrum of plane Couette flow UCM liquid with $We=10$ and $\alpha=1$. Using the original matrices solving a GEVP with 125 elements and also using the transformations and solving a EVP with 500 and 800 elements.

The predicted spectrum is composed by the two discrete eigenvalues, the GL modes, and a set of eigenvalues that approximate the continuous part of the spectrum. The computed GL modes agree well with those predicted by Sureshkumar (2004) , using streamfunction formulation and spectral method. As in the spectral method predictions of Sureshkumar (2004) and Wilson *et. al.* (1999), the approximation of the continuous spectrum is not precise. The predictions obtained with the primitive variable formulation and the set of finite element basis functions used to expand the unknown fields show that the approximation to the continuous spectrum can be divided into three sets of eigenvalues. One set of eigenvalues approximate well the analytical solution of the problem, i.e. they lie near the line segment $-1/We\pm i\alpha$. The

number of eigenvalues aligned near the analytical solution is equal the number of nodes of the mesh and their imaginary part coincide with the coordinates of the nodes.

The other two sets are similar to those predicted by the streamfunction formulation and spectral methods, they form an oval shape figure around the analytical solution. In a way that is not clear, the linear stability analysis formulation based on finite element basis functions was able to capture well the continuous part of the spectrum, together with the oval shape figure predicted by the spectral method results.

The effect of the level of discretization on the computed eigenvalues is presented in Fig.7. Three different meshes were tested: 125, 500 and 800 elements. The two discrete eigenvalues are converged with the number of elements. As in the predictions of Sureshkumar (2004) and Wilson *et. al.* (1999), the two branches that form the oval-shaped figure slowly converge to the analytical solution as the number of element rises. With 800 elements, the relative error of the approximations to the continuous part of the spectrum is less than 4%.

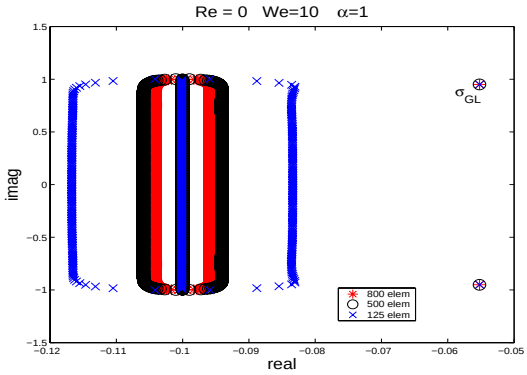

Figure 7. Spectrum of plane Couette flow UCM liquid with $We = 10$ and $\alpha = 1$. Using the original matrices solving a GEVP with 125 elements and also using the transformations and solving a EVP with 500 and 800 elements.

The method presented in this work reduces significantly the time of computation of memory requirement to solve the eigenspectrum of viscoelastic flows. As mention before, the proposed transformations create a simple EVP, which size is approximately $1/5$ of the original GEVP, such that its eigenvalues correspond to finite eigenvalues of the original problem. Table 1 presents size (number of degrees of freedom of the problem) and the CPU time, in seconds, required to solve the original GEVP t_{GEVP} and to solve the reduced EVP t_{EVP} for different meshes. The later includes the time to compute all operations necessary to obtain the reduced EVP.

Table 1. Number of elements matrices sizes and CPU time, in seconds, required to compute the eigenvalues by the different methods: (a) solving the original GEVP by QZ method; (b) solving the reduced EVP using LAPACK routine.

# ele	N_{dof} GEVP	N_{dof} EVP	t_{GEVP} [s]	t_{EVP} [s]	t_{GEVP}/t_{EVP}
60	1202	242	140	3.1	45
100	2002	402	629	13	48
125	2502	502	1252	21	59
150	3002	602	—	43.6	—
200	4002	802	—	85.8	—
300	6002	1202	—	254.3	—

The sub-block matrices involved in the algorithm are sparse. All the matrix operations take advantage of the matrix structure. The proposed method is significantly faster than the solution of the full GEVP by QZ method. The speed-up factor is approximately equal to 50. It is important to notice that there is no approximation in the proposed method. It only takes advantage of the structure of the matrices to eliminate the infinite eigenvalues of the problem. It is not limited to any particular constitutive model and may be extended to two-dimensional flows and other discretization methods besides the Galerkin's / finite element method used here.

3. FINAL REMARKS

This work presents a finite element formulation for the solution of linear stability analysis of a plane Couette flow of an UCM liquid. In a way that is not clear, the computed eigenspectrum seems to give a better approximation of the

continuous part of the spectrum, when compared to the available predictions obtained with streamfunction formulation and spectral methods.

A new method to eliminate the infinite eigenvalues of the generalized eigenvalue problem is also presented. The algorithm transforms the original generalized eigenproblem (GEVP) into an equivalent simple eigenvalue problem (EVP), whose dimension is approximately $1/5$ of the original problem. The eigenvalues of the transformed EVP correspond exactly to the finite eigenvalues of the original GEVP.

In the example presented here, the proposed method was faster by an order of magnitude (factor of approximately 50) when compared to the solution of the original GEVP.

4. ACKNOWLEDGEMENTS

This work was funded by grants from the Brazilian Research Council (CNPq) and the Science Foundation of State of Rio de Janeiro (FAPERJ).

J. V. Valério would like to thank Prof. L.E.Scriven and J. M. de Santos for discussions and encouragement during her stay at the University of Minnesota.

5. REFERENCES

Gorodtsov, V. A. and Leonov, A. I., 1967, "On a linear instability of plane Couette flow of viscoelastic fluid." *J. Appl. Math. Mech.* $\mathbf{31}, 310 - 319$.

Renardy, M. and Renardy, Y., 1986, "Linear stability of plane Couette flow of an upper convected Maxwell fluid." *J. Non-Newtonian Fluid Mech.* $\mathbf{22}, 23 - 33$.

Rouse, P. E. [1953] A theory of the linear viscoelastic properties of dilute solutions of coiling polymers. *J. Chem. Phys.* $\mathbf{21}, 1272 - 1280$.

Sureshkumar, R., 2004, "Stability analysis using compressible viscoelastic formulations." *J. Non-Newtonian Fluid Mech.* $\mathbf{116}, 471 - 477$.

Sureshkumar, R. and Arora,K., 2002, "Efficient computation of the eigenspectrum of viscoelastic flows using submatrix-based transformation of the linerized equations." *J. Non-Newtonian Fluid Mech.* $\mathbf{104}, 75 - 85$.

Sureshkumar, R. and Beris, A. N. 1995, "Linear stability analysis of viscoelastic Poiseuille flow using an Arnoldi-based orthogonalization algorithm." *J. Non-Newtonian Fluid Mech.* $\mathbf{56}, 151 - 182$.

Sureshkumar, R., Smith, M. D., Armstrong, R. C. and Brown, R. A., 1999, "Linear stability and dynamic of viscoelastic flows using time-dependent numerical simulations." *J. Non-Newtonian Fluid Mech.* $\mathbf{82}, 57 - 104$.

Wilson, H. J., Renardy, M. and Renardy, Y., 1999, "Structure of the spectrum in zero Reynolds number shear flow of the UCM and Odroyd-B liquids." *J. Non-Newtonian Fluid Mech.* $\mathbf{80}, 251 - 268$.

Grillet, A. M. and Yang, B. and Khomami, B. and Shaqfeh, S. G., E.M., 1999, "Modeling of viscoelastic lid-driven cavity flow using finite element simulations", *J. Non-Newtonian Fluid Mech.* $\mathbf{88}, 99 - 131$.

Kupferman, R., 2005, "On the linear stability o plane Couette flow for an Oldroid-B fluid and its numerical approximation", *J. Non-Newtonian Fluid Mech.* $\mathbf{127}, 169 - 190$.

Szady, M. J. and Salomon, T. R. and Liu, A. W. and Bornside, D. E. and Armstrong, R. C. and Brown, R. A., 1995, "A new mixed finite element method for viscoelastic flows governed by diferential contitutive equations", *J. Non-Newtonian Fluid Mech.* $\mathbf{59}, 215 - 243$.

Pasquali, M. and Scriven, L. E., 2002, "Free surface flows of polymer solutions with mod- els based on the conformation tensor", *J. Non-Newtonian Fluid Mech.* $\mathbf{108}, 363 - 400$.

6. Responsibility notice

The author(s) is (are) the only responsible for the printed material included in this paper